Numerical Inversion and Modeling of 1993–97 Deformation Data at Mount Etna (Italy)

E. Trasatti*, N. Piana Agostinetti*, S.Cianetti*,
C. Giunchi*, A. Bonaccorso** & M. Bonafede***
trasatti@ingv.it, piana@ingv.it, cianetti@ingv.it

Istituto Nazionale di Geofisica e Vulcanologia
* Sismologia e Tettonofisica
Via di Vigna Murata, 605
I - 00143 ROMA
** Sezione di Catania
Piazza Roma, 2
I - 95125 CATANIA

*** Dipartimento di Fisica, Settore Geofisica
Università di Bologna
Viale Berti Pichat 8
I - 40127 BOLOGNA

9th International Workshop on Numerical Modeling of Mantle Convection and Lithospheric Dynamics,
EMFCSC, Erice, Sicily (Italy), 8 – 14 September 2005

Abstract

Since 1993 geodetic data obtained by different techniques (GPS, EDM, SAR, leveling) detected a consistent inflation of the Mt. Etna volcano. The inflation, culminated with the 1998–2001 strong explosive activity from summit craters and recent 2001 and 2002 flank eruptions, may be interpreted by magma ascent and re-filling of the volcanic plumbing system and reservoirs. We model the 1993–97 GPS data by pressurized sources simulating the magma reservoir using a 3D Finite Element modeling coupled to a Monte Carlo inversion. The power of this technique, if compared with analytical inversions, is that sources can be placed in complex media (heterogeneous, with topography, inelastic etc.) so that the inversion result is not influenced by the usual approximations of elastic, homogeneous half-space. The FE model of Mt. Etna is characterized by a regular mesh below the volcanic edifice, and by arbitrarily distorted brick elements elsewhere. The potential point sources are contained in a specified volume of elements, and located below the summit craters. We compute the solutions at GPS observation points for each potential source and for each stress component. Source parameters are obtained as a linear combination of the 6 independent stress components. We consider four classes of models characterized by topography/flat free surface and homogeneous/heterogeneous medium, finding the best-fit source for each model.

GPS Data of 1993–97 Inflation

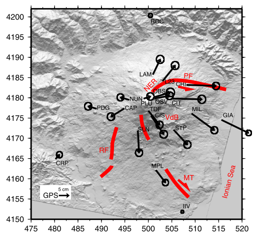

The dataset is composed of 20 GPS displacement measurements. Data have been collected between 1993 and 1997. The deformation data detect a consistent inflation of the volcanic edifice. The red lines show the major surface fault systems bordering the eastern and southern sectors of the volcano (NER = North East Rift, PF = Pernicana fault, MT = Mascalucia Trecastagni fault; RF = Ragalna fault; VdB = Valle del Bove).

Finite Element Modelling & Inversion

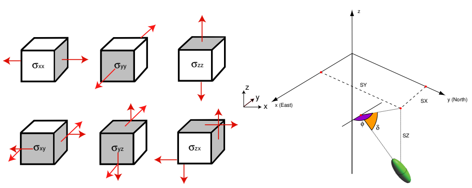

We model the inflation by a deep volcanic source, considered as point-source. The source intensity is given by its stress tensor, identifying an ellipsoidal pressure source. The solution is a weighted combination of displacements due to the 6 elementary sources depicted in Figure.

The FE models of Mt. Etna are characterized by a regular element grid, spaced every 400 m and placed below the volcanic edifice, and by arbitrarily distorted brick elements elsewhere (60000 elements). The potential sources are contained in a volume of $10\times10\times10$ elements, approximately below the summit craters, between 3 km and 7 km b.s.l.. The whole model measures $150\times150\times80$ km and the Mt. Etna topography has an extension of 40×40 km with increased resolution.

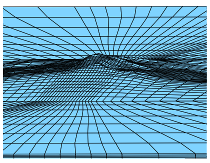

The input of the inversion is a matrix of 6000 solutions consisting in the surface deformation computed at GPS sites for each element and for each stress component. The inversion is performed by means of the Neighbourhood Algorithm technique (*Sambridge, 1999*). From the inversion we retrieve 9 parameters: the source position and the scale factors of the stress components.

We consider four classes of models in which the sources act, whose characteristics are shown in the table.

Model	Surface	Rigidity
HOF	flat	homogeneous
HOT	topography	homogeneous
HEF	flat	heterogeneous
HET	topography	heterogeneous

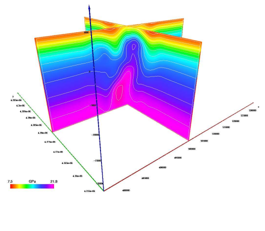

Rigidity contrasts inside Mt.Etna are computed from V_p velocity anomalies by *Chiarabba & al., 2000*, assuming a Poissonian medium and a constant density ρ = 2500 kg/m^3. In the homogeneous models the rigidity is fixed at 1 GPa while seismic derived rigidities range between 7.5 GPa and 21.9 GPa.

Result 1: Synthetic test

Synthetic tests for spherical/ellipsoidal sources are performed, obtaining best-fit models with a χ^2 misfit as low as 0.1 and 0.001 respectively. The NA method is able to solve the ambiguity of 3D orientation of the sphere axis.

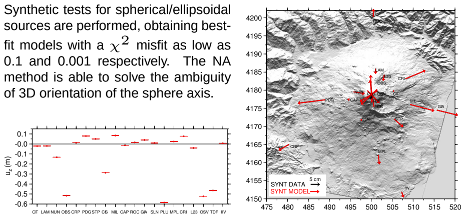

Result 2: Source Parameters

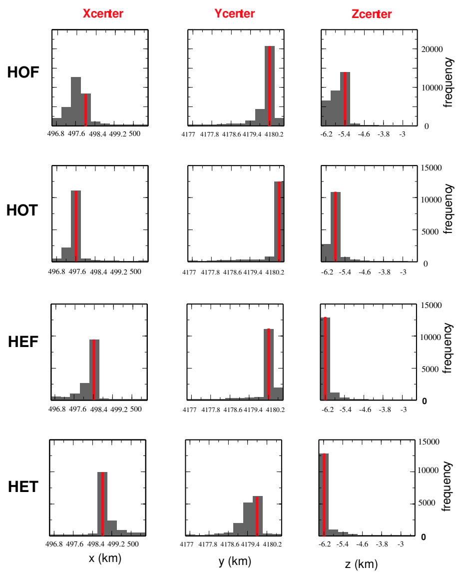

Best-fit source positions are indicated in red; the histogram bin corresponds to the element size (400 m). The source centers are located at North West of the summit craters. Slight differences are found in the models presented. The topography and the heterogeneities cause a deepening of the source since its depth b.s.l. is 5.4 km in model HOF, 5.8 km in HOT and 6.2 km in HEF and HET.

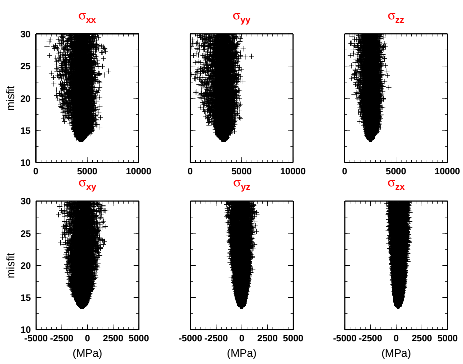

We show the misfit for stress components of model HOF, while similar results are obtained with models HOT, HEF and HET. The models are characterized by a χ^2 misfit ranging between 12.8 and 14.3. There is a trade-off between volume and overpressure of the ellipsoidal body, because of the point-source approximation. If we suppose a source volume V$\simeq$ 3 km^3 (e.g. *Bonaccorso & al., 2005*), the overpressure acting within the source in model HOF is $\triangle P\ \simeq$ 20-30 MPa, in agreement with values commonly adopted in volcanic modeling.

It must be noted that varying the search parameters in NA, the results obtained can slightly differ. This is due to the reduced dataset, unable to constrain univocally the source unknown parameters. Greater uncertainties are found in the source position, while the stress tensor is solved much better.

Model	δ (deg)	ϕ (deg)
HOF	84	184
HOT	78	118
HEF	83	135
HET	83	155

The orientation of the pressure source is very similar in all the models presented. We find evidence of a vertically elongated body, dipping East – South Est.

Result 3: Computed deformation

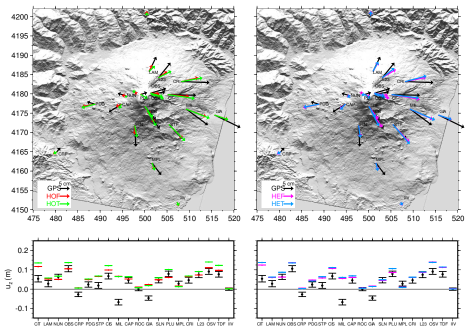

The best models fit the displacement in a similar way. The overall pattern of computed horizontal deformation resembles the radial pattern of measured displacement. The vertical displacement always overestimate the observations, but the computed trend matches the data. All the models fail to predict the negative vertical displacement recorded at MIL and GIA, probably caused by subsidence and eastward sliding of SE sector of Mt. Etna.

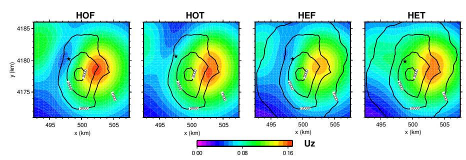

The vertical displacement generated by the 4 sources inverted is very similar, confirming the good predictions for the observed data.

Conclusions

♡ **We present the results of the first 3D FE modeling coupled to a NA inversion. This is just a preliminary test to show the possibility to account for realistic features such as topography and heterogeneities, applied to volcanic regions.**

♣ **Good results from synthetic tests, performed on spherical/ellipsoidal sources, confirm the robustness of the method to invert real deformation data.**

♢ **Results from GPS data inversion show evidence for a vertically elongated body, located approximately North West of the summit craters. This result is a robust feature of the inversions, since it is common to models with /without topography and with/without rigidity contrasts.**

♠ **Topography and heterogeneities provide minor perturbations to the position and orientation of the body, as evidenced by the similar statistical performance of the models considered.**

References

Bonaccorso A., Cianetti S., Giunchi C., Trasatti E., Bonafede M. & Boschi E., 2005, Analytical and 3D numerical modeling of Mt. Etna (Italy) volcano inflation, *Geophys.J.Int.*, in press.
Chiarabba, C., A. Amato, F. Barberi & E. Boschi, 2000, Recent seismic tomographic modelling of the Mt. Etna plumbing system, *J.Geophys.Res.*, **105(B5)**, 10,923–10,938.
Sambridge, M., 1999, Geophysical inversion with a neighbourhood algorithm – I. Searching a parameter space, *Geophys.J.Int.*, **138**, 479–494.